

Synthesis, characterization, photophysical studies and interaction with DNA of a new family Ru(II) Furyl- and Thienyl-imidazo-phenanthroline polypyridyl complexes.

**Bruno Pedras,^{1,2*} Rosa M. F. Batista,³ Laura Tormo,⁴ Susana P. G. Costa,³
M. Manuela M. Raposo,^{3*} Guillermo Orellana,^{4*} José Luís Capelo,^{1,2}
Carlos Lodeiro.^{1*}**

¹ *Grupo BIOSCOPE, Departamento de Química-Física, Facultad de Ciencias de Ourense, Universidad de Vigo, Campus de Ourense, E32004, Spain.*

² *REQUIMTE, Departamento de Química, FCT-UNL, 2829-516 Caparica, Portugal.*

³ *Centro de Química, Universidade do Minho, Campus de Gualtar, 4710-057, Portugal*

⁴ *Departamento de Química Orgánica I, Facultad de Química, Universidad Complutense de Madrid, E-28040 Madrid, Spain*

*Authors to whom correspondence should be addressed. E-mail:
b.pedras@dq.fct.unl.pt Fax: +351 212 948 385 (B.P.); E-mail:
mfox@quimica.uminho.pt Fax: +351 253 604382 (M.M.M.R.); E-mail:
orellana@quim.ucm.es Fax: +34 91 394 4103 (GO); E-mail:
clodeiro@uvigo.es Fax: + 34 988 387001 (C. L.)

Abstract

A new family of Ru(II) polypyridyl complexes (**C1** to **C6**) containing furyl- or thienyl-imidazo-phenanthroline ligands (4-6) were synthesized using microwave irradiation and characterized by elemental analysis, ¹H-NMR, UV-vis absorption and fluorescence spectroscopy, FAB, EI-MS and MALDI-TOF-MS spectrometry. On the other hand, the novel furyl- or thienyl-imidazo-phenanthroline derivatives (5-6) were synthesized through the Radziszewski reaction and completely characterized by the usual spectroscopic techniques. The interaction of the complexes with calf thymus DNA in the absence and in the presence of different quenchers (ethidium bromide, potassium hexacyanoferrate(II) and methylviologen) has been studied by absorption spectroscopy, steady-state and single-photon timing luminescence measurements. Their electronic spectra show visible absorption peaks at 457-463 nm, with red luminescence at 603-613 nm. The emission quantum yields of these complexes are between 0.006–0.016 in air-equilibrated DMSO solution. Luminescence lifetimes in water lie within the 0.4 to 1.0 μs range, with a non-exponential behavior due to aggregation of the probe. Ru(II) complexes **C3**, **C4**, **C5** and **C6** show intrinsic dsDNA-binding constants of 2.74×10^5 , 3.02×10^5 , 1.32×10^5 and $1.63 \times 10^5 \text{ M}^{-1}$, respectively. The planar extended structure of the imidazo-phenanthroline ligands and the collected spectroscopic data suggest a partial intercalative binding mode of the novel metal probes to double-stranded DNA.

Keywords: Ru(II) complexes , DNA, Phenanthroline, Thiophene, Furan.

Introduction

Among the multiple application fields of ruthenium(II) polypyridyl complexes,¹ its interaction with nucleic acids has been one of the most thoroughly studied over more than two decades.² Featuring a unique set of chemical properties such as stability, excited-state reactivity, redox potentials,³ luminescence and excited state lifetimes, these complexes have attracted considerable attention from a great number of researchers, finding applications in areas such as photophysics, photochemistry, supramolecular chemistry, bioinorganic chemistry and catalysis.

Concerning their interaction with biological structures, Ru(II) polyazaheteroaromatic compounds have been used as probes of the biopolymer tertiary structure, photocleavage agents and, in recent times, as inhibitors of biological functions.^{4,1a} One of the most extensively studied metal complexes used as luminescent probe is $[\text{Ru}(\text{bpy})_2(\text{dppz})]^{2+}$ (bpy = 2,2'-bipyridine, dppz = dipyrido[3,2-a:2',3'-c]phenazine).⁵ This complex functions as a molecular "light switch" for DNA because of the dramatic emission enhancement experienced by this probe and related phenazine complexes in the presence of double-stranded nucleic acids, being otherwise weakly emissive in aqueous solution. The reason for this behaviour is the peculiar electronic nature of the phenazine ligand and the lowest-lying excited state swap that occurs in protic solvents,⁶ together with the intercalative binding mode to double-stranded DNA of Ru(II)-dppz and related complexes.⁷ For all ruthenium(II) polypyridyl complexes, non-radiative vibrational deactivation with the water molecules can be minimized by a close interaction with a hydrophobic negatively charged surface,⁸ and the intimate contact (e.g. DNA intercalation)

with the biopolymer protects the triplet excited state of the probe from the O₂ quenching,⁹ overall leading to a substantial increase in the ³MLCT excited state lifetime.

Very recently these complexes have been applied as multifunctional biological agents for direct imaging of DNA in living cells.¹⁰ By varying the ligands that constitute the complexes, it is possible to modify the nature and strength of their binding to nucleic acids. As mentioned above, all positively charged complexes are expected to be attracted to the anionic DNA, and those containing at least one extended heteroaromatic ligand in the coordination sphere may insert such ligand between adjacent base-pairs of double-stranded DNA (i.e. binding by intercalation).^{2a,7,9a,11} Indeed, it has been observed that while [Ru(bpy)₃]²⁺ binds in a relatively weak manner to DNA (mostly through electrostatic interaction in one of the grooves), the interaction of [Ru(phen)₃]²⁺ is stronger.¹²

Therefore, in order to study the factors that influence the DNA-binding mode of Ru(II) complexes with extended and ancillary ligands, the structural diversity of the metal chelating structures must be taken into account. Moreover, a further tuning of the probe photophysical and DNA binding properties might be achieved when new extended conjugation systems are composed by different heterocyclic nuclei (molecular *meccano* concept).

Following our ongoing projects on fluorescent reporters and their sensing applications,¹³ we have tackled the synthesis and characterization of novel (oligo)thienyl-¹⁴ and arylthienyl-imidazo-phenanthrolines¹⁵ due to their interesting emissive properties (see below). Taking also into account that furans exhibit high fluorescence quantum yields¹⁶ and the recent studies concerning the DNA binding and photocleavage of Ru(II) complexes of a 2-(5-methyl-furan-

2-yl)imidazo[4,5-f][1,10]phenanthroline ligand,¹⁷ suggesting that these complexes bind to DNA through intercalation and, when irradiated at 400 nm, promote the photocleavage of the DNA, we set out to synthesize Ru(II) furyl-imidazo-phenanthroline complexes that were hitherto unknown.

In this way, four new ligands and six Ru(II) polypyridyl complexes, **C1** to **C6**, are photophysically characterized in this work, and the interaction of the latter with calf-thymus DNA has been followed by steady-state and single-photon timing luminescence measurements. The effect of three different quenchers on the emission properties of the DNA-bound complexes has also been studied, in an attempt to reveal the possible binding modes of the complexes to the nucleic acid.¹⁸

Experimental Section

Materials. All reagents used in the present work were commercially available and used without further purification, unless otherwise stated. Progress of the reactions was monitored by thin layer chromatography (0.25 mm thick pre-coated Merck Fertigplatten Kieselgel 60F₂₅₄ silica plates), while purification was carried out by silica gel column chromatography (Merck Kieselgel 60; 230-400 mesh). Calf thymus DNA was obtained from Pharmacia GE Healthcare and purified by extensive dialysis against TRIS buffer. The concentration of stock solutions was determined spectrophotometrically using the molar absorption coefficient per base pair ($12800 \text{ M}^{-1} \text{ cm}^{-1}$) at $258 \text{ nm}^{\text{9a}}$ and found to be 2.82 mM (for the stock solution used with **C1** to **C3**) and 2.02 mM (for the stock solution used with **C4** to **C6**) in base pairs. All the experiments with DNA were carried out in pH-7.0 3-mM Tris buffer.

Instrumentation. NMR spectra of the ligands were obtained on a Varian Unity Plus spectrometer at 300 MHz for ^1H NMR and 75.4 MHz for ^{13}C NMR or a Bruker Avance III 400 at 400 MHz for ^1H NMR and 100 MHz for ^{13}C NMR, using the solvent residual peak as internal reference. The solvents are indicated in parenthesis before the chemical shift values (δ in ppm relative to TMS). NMR spectra of the complexes were recorded on a Bruker AVANCE II at 400 MHz for ^1H NMR, and processed with the TOPSPIN 2.0 software (Bruker). Melting points were determined on a Gallenkamp apparatus and are uncorrected. Infrared spectra were recorded on a BOMEM MB 104 spectrophotometer. UV-vis absorption spectra of the ligands (200–800 nm) were measured with a Shimadzu UV/2501PC apparatus and those of the complexes on a Varian Cary 3Bio spectrophotometer.

Mass spectrometry analyses of the ligands were performed at the C.A.C.T.I. - Unidad de Espectrometria de Masas of the University of Vigo, Spain. MALDI-TOF-MS spectra have been performed in a MALDI-TOF-MS model Voyager DE-PRO Biospectrometry Workstation equipped with a nitrogen laser radiating at 337 nm from Applied Biosystems (Foster City, United States) from the MALDI-TOF-MS Service of the REQUIMTE, Chemistry Department, Universidade Nova de Lisboa and in the MALDI-TOF-MS-MS model 4700 Applied Biosystems at the Faculty of Science of Ourense, University of Vigo. The acceleration voltage was 2.0×10^4 kV with a delayed extraction (DE) time of 200 ns. The spectra represent accumulations of 5 x 100 laser shots. The reflection mode was used. The ion source and flight tube pressures were less than 1.80×10^{-7} and 5.60×10^{-8} Torr, respectively.

The MALDI mass spectra of the soluble compounds (1 or 2 $\mu\text{g}/\mu\text{L}$) were recorded using the conventional sample preparation method for MALDI-MS without other MALDI matrix.

Elemental analyses were performed at the Analytical Services of the Laboratory of REQUIMTE-Departamento de Química, Universidade Nova de Lisboa, on a Thermo Finnigan-CE Flash-EA 1112-CHNS Instrument.

The steady-state luminescence measurements were carried out with a Perkin-Elmer LS-5 spectrofluorometer. Luminescence lifetimes were determined at 25 ± 1 °C using ca. 10^{-5} M solutions of the Ru(II) complexes by the single-photon timing (SPT) technique with an Edinburgh Analytical Instruments LP900 kinetic spectrometer. Excitation of the samples was carried out with a Horiba NanoLED-07N 405-nm pulsed laser diode (<700 ps). A wide band-pass 405-nm interference filter (Edmund Scientific) was placed in front of the laser source and cut-off filters (590 nm, Lambda Research Optics) were used in the emission path to avoid distortions from the laser light scattering. The luminescence decay profiles were fit either to a single exponential function or to a sum of 2-3 exponential functions with the original Marquardt algorithm-based EAI decay analysis software. Satisfactory fits were obtained in all cases, as judged from the weighted residuals, the goodness-of-the-fit χ^2 parameter and the autocorrelation function. No oxygen outgassing was performed. The accuracy in the measured lifetimes for the multi-exponential decay fits is estimated to be $\pm 3\%$ (1% for the single-exponential decays) and 10% for the relative weights. The pre-exponential weighted emission lifetime (τ_m) is defined according to Eq. 1, where τ_i is the emission lifetime for each component of the multi-exponential fit whose relative weight is $(\%)_i$.

$$\tau_m = \sum_i \frac{(\%)_i}{100} \tau_i \quad (1)$$

For the preliminary studies of complexes C1 to C3 in the presence of DNA, a solution of the metal complex in TRIS buffer with a concentration of ca. 10^{-5} M was obtained by dilution of a concentrated DMSO stock solution of each complex. Each solution was mixed with DNA in different proportions, and their spectra recorded both in the presence and in the absence of the biopolymer. The mixtures were allowed to equilibrate for at least half an hour between each addition and the respective measurement. For the subsequent studies with DNA the same procedure was adopted, by measuring at different [DNA]/[Ru] ratios and choosing the ratio after which no significant changes in the emission spectrum and lifetime were observed to be studied with the selected quenchers (ethidium bromide, potassium hexacyanoferrate(II) and methyl viologen).

Synthesis. The precursor complex, namely *cis*-[Ru(bpy)₂Cl₂], was synthesized according to literature methods.¹⁹ The syntheses of ligands 4a and 4b have been previously reported.^{14a}

Insert Scheme 1 at about here

General procedure for the synthesis of imidazo[4,5-*f*][1,10]phenanthrolines 5 and 6

A mixture of the corresponding aldehyde (1.2 mmol), NH₄OAc (20 mmol) and 1,10-phenanthroline-5,6-dione (1 mmol) in glacial acetic acid (10 mL) was stirred and heated at reflux for 5 h. The mixture was then cooled to room

temperature and the product precipitated during neutralization with NH_4OH 5 M. The precipitate was filtered out, washed with water and diethyl ether, recrystallized from absolute ethanol and dried under vacuum to give the expected product.

2-(4'-(thien-2''-yl)phen-2'-yl)-1*H*-imidazo[4,5-*f*][1,10]phenanthroline (5).

Yellow solid (0.139 g, 82%). ^1H NMR (300 MHz, $\text{DMSO-}d_6$): δ 7.18-7.21 (m, 1H, 4''-H), 7.62 (d, 1H, $J = 5.1$ Hz, 3''-H), 7.66 (d, 1H, $J = 3.6$ Hz, 5''-H), 7.81-7.85 (m, 2H, 5-H and 10-H), 7.90 (d, 2H, $J = 8.7$ Hz, 2'-H and 6'-H), 8.31 (d, 2H, $J = 8.4$ Hz, 3'-H and 5'-H), 8.92 (dd, 2H, $J = 8.1$ and 1.5 Hz, 4-H and 11-H), 9.03 (dd, 2H, $J = 4.5$ and 1.8 Hz, 6-H and 9-H), 13.79 (s, 1H, *NH*) ppm. ^{13}C NMR (75.4 MHz, $\text{DMSO-}d_6$): δ 123.4, 124.5, 125.8, 126.5, 126.9, 128.7, 128.8, 129.8, 134.7, 135.9, 142.6, 146.4, 147.8, 150.1 ppm. MS (FAB): m/z (%) 379 ($[\text{M}+\text{H}]^+$, 100). HRMS (FAB): m/z calcd. for $\text{C}_{23}\text{H}_{15}\text{N}_4\text{S}$ 379.1017; found 379.1015. IR (KBr, ν/cm^{-1}): 3439, 2950, 1605, 1562, 1531, 1479, 1451, 1429, 1395, 1351, 1312, 1296, 1259, 1212, 1190, 1119, 1069, 1029, 957, 844, 803, 740. Decomposition at $T > 320$ °C. UV (ethanol, nm): λ_{max} ($\log \epsilon$) = 345 (4.16).

2-(furan-2'-yl)-1*H*-imidazo[4,5-*f*][1,10]phenanthroline (6a). The compound

was isolated as an orange solid (0.114 g, 85%). ^1H NMR (300 MHz, $\text{DMSO-}d_6$): δ 6.76-6.79 (m, 1H, 4'-H), 7.25 (d, 1H, $J = 3.0$ Hz, 3'-H), 7.78-7.82 (m, 2H, 5-H + 10-H), 7.99 (d, 1H, $J = 1.2$ Hz, 5'-H), 8.90 (d, 2H, $J = 7.8$ Hz, 4-H + 11-H), 9.02 (d, 2H, $J = 1.8$ Hz, 6-H + 9-H), 13.93 (br s, 1H, *NH*) ppm. ^{13}C NMR (75.4 MHz, $\text{DMSO-}d_6$): δ 109.9, 112.5, 123.3, 129.6, 143.0, 143.6, 144.4, 145.4, 147.9 ppm. MS (FAB): m/z (%) 287 ($[\text{M}+\text{H}]^+$, 100), 226 (5). HRMS (FAB): m/z

calcd. for C₁₇H₁₁N₄O 287.09389; found 287.09274. IR (Nujol, ν /cm⁻¹): 3396, 2923, 2853, 1644, 1565, 1538, 1507, 1463, 1397, 1377, 1350, 1228, 1191, 1116, 1073, 1017, 976, 897, 885, 807, 739. Mp = 122.3–124.5 °C. UV/Vis (ethanol, nm): λ_{\max} (log ϵ) = 318 (4.14).

2-(5'-(thien-2''-yl)furan-2'-yl)-1H-imidazo[4,5-f][1,10]phenanthroline (6b).

The compound was isolated as a dark yellow solid (0.110 g, 79 %). ¹H NMR (400 MHz, DMSO-*d*₆): δ 7.03 (d, 1H, *J* = 3.6 Hz, 3'-H), 7.20-7.22 (m, 1H, 4''-H), 7.33 (d, 1H, *J* = 4.0 Hz, 4'-H), 7.60 (dd, 1H, *J* = 3.6 and 1.2 Hz, 3''-H), 7.66 (dd, 1H, *J* = 5.2 and 0.8 Hz, 5''-H), 7.79-7.86 (m, 2H, 5-H + 10-H), 8.89-8.94 (m, 2H, 4-H + 11-H), 9.03 (dd, 2H, *J* = 4.0 and 2.0 Hz, 6-H + 9-H), 13.89 (s, 1H, NH) ppm. ¹³C NMR (100.6 MHz, DMSO-*d*₆): δ 108.0, 112.3, 119.2, 123.1, 123.4, 123.5, 124.4, 125.9, 126.4, 128.3, 129.7, 131.9, 135.8, 142.5, 143.6, 143.7, 144.3, 147.9, 147.9, 149.8 ppm. MS (FAB): *m/z* (%) 369 ([M+H]⁺, 100), 226 (4). HRMS (FAB): *m/z* calcd. for C₂₁H₁₂N₄OS 369.08048; found 369.08046. IR (Liquid film, ν /cm⁻¹): 3436, 1567, 1498, 1444, 1421, 1265, 1072, 1017, 896, 738, 704. Mp = 241.0-242.2 °C. UV/Vis (ethanol, nm): λ_{\max} (log ϵ) = 364 (4.20).

2-(5'-phenylfuran-2'-yl)-1H-imidazo[4,5-f][1,10]phenanthroline (6c).

The compound was isolated as a yellow solid (0.061 g, 60 %). ¹H NMR (400 MHz, DMSO-*d*₆): δ 7.23 (d, 1H, *J* = 3.6 Hz, 3'-H), 7.34-7.38 (m, 2H, 4''-H + 4'-H), 7.49 (t, 2H, *J* = 8.0 and 7.6 Hz, 3''-H + 5''-H), 7.80-7.83 (m, 2H, 5-H + 10-H), 7.91 (d, 2H, *J* = 7.6 Hz, 2''-H + 6''-H), 8.93 (dd, 2H, *J* = 8.4 and 1.6 Hz, 4-H + 11-H), 9.02 (dd, 2H, *J* = 6.0 and 1.6 Hz, 6-H + 9-H) ppm. ¹³C NMR (100.6 MHz, DMSO-*d*₆): δ 108.4, 111.9, 121.6, 123.3, 123.9, 128.1, 128.9, 131.3, 131.3,

143.2, 143.6, 145.3, 147.8, 153.9 ppm. MS (FAB): m/z (%) 363 ($[M+H]^+$, 100). HRMS (FAB): m/z calcd. for $C_{23}H_{15}N_4O$ 363.12380; found 363.12404. IR (Nujol, ν/cm^{-1}): 3371, 2911, 2853, 1619, 1565, 1490, 1397, 1299, 1277, 1190, 1150, 1124, 1073, 1027, 924, 803, 758, 688. Mp = 243.4-244.9. UV/Vis (ethanol, nm): λ_{max} (log ϵ) = 353 (4.48).

Synthesis of the Ru(II) Complexes. In 5 mL of ethylene glycol, the corresponding quantity of imidazo-phenanthroline ligand and the $Ru(bpy)_2Cl_2$ complex were dissolved. The mixture was heated in a Milestone microwave oven (450 W) for 30 s, which led to a color change from violet to deep orange, and then allowed to cool for a while. The mixture was heated for three more periods of 30 s. The solvent was removed by distillation at low pressure, the residue was dissolved in 2 mL of water, and a saturated NH_4PF_6 aqueous solution was added. The precipitate formed was then filtered through a frit, washed with water (3 x 10 mL) and diethyl ether (3 x 10 mL), and dried under vacuum.

C1: 30.2 mg (7.85×10^{-5} mol) of **4a** and 42.7 mg (8.2×10^{-5} mol) of $Ru(bpy)_2Cl_2$ were used. Colour: Deep orange. Yield: 73.9 mg (87%). Anal. Calcd for $C_{41}H_{28}F_{12}N_8P_2RuS_2$: C, 45.30; H, 2.60; N, 10.30; S, 5.90. Found: C, 45.40; H, 2.80; N, 10.05; S, 5.85. 1H NMR (CD_3CN): δ = 8.69 (s, 1H); 8.56 (t, 4H); 8.36 (d, 2H); 8.11 (m, 4H); 7.85 (m, 7H); 7.47 (m, 7H); 7.13 (m, 3H) ppm. FD-MS: m/z 943.06 ($[M-PF_6]^+$), 797.08 ($[M-2PF_6-H]^+$), 399.04 ($[M-2PF_6]^{2+}$). ESI-MS: m/z 943.2 ($[M-PF_6]^+$), 797.2 ($[M-2PF_6-H]^+$), 399.1 ($[M-2PF_6]^{2+}$). MALDI-TOF MS: m/z 797.6 ($[M-2PF_6-H]^+$), 641.6 ($[M-2PF_6-bpy-H]^+$).

C2: 24.3 mg (5.85×10^{-5} mol) of **4b** and 32.0 mg (6.15×10^{-5} mol) of Ru(bpy)₂Cl₂ were used. A few drops of ethanol were added in order to increase solubilization of the ligand. Colour: Deep orange. Yield: 29.3 mg (45%). Anal. Calcd for C₄₂H₃₀F₁₂N₈OP₂RuS₂·1.5C₂H₅OH: C, 45.55; H, 3.30; N, 9.45; S, 5.40. Found: C, 45.88; H, 3.40; N, 9.70; S, 5.85. ¹H NMR (CD₃CN): δ = 8.80 (d, 2H); 8.53 (m, 4H); 8.10 (t, 2H); 7.99 (t, 2H); 7.87 (m, 4H); 7.66 (d, 3H); 7.56 (m, 2H); 7.44 (t, 2H); 7.25 (t, 2H); 7.02 (d, 1H); 6.91 (d, 1H); 6.24 (d, 1H); 3.92 (s, 3H) ppm. FD-MS: *m/z* 973.03 ([M-PF₆]⁺), 827.07 ([M-2PF₆-H]⁺). ESI-MS: *m/z* 973.2 ([M-PF₆]⁺), 827.2 ([M-2PF₆-H]⁺), 414.1 ([M-Ru(bpy)₂(PF₆)₂]⁺). MALDI-TOF MS: *m/z* 827.6 ([M-2PF₆-H]⁺).

C3: 30.5 mg (8.06×10^{-5} mol) of **5** and 44.1 mg (8.47×10^{-5} mol) of Ru(bpy)₂Cl₂ were used. Colour: Deep orange. Yield: 26.3 mg (30%). Anal. Calcd for C₄₃H₃₀F₁₂N₈P₂RuS·6H₂O: C, 43.40; H, 3.55; N, 9.40; S, 2.70. Found: C, 43.35; H, 3.25; N, 9.40; S, 2.55. ¹H NMR ((CD₃)₂CO): δ = 9.21 (d, 2H); 8.89 (dd, 4H); 8.50 (d, 2H); 8.31 (m, 4H); 8.20 (m, 4H); 7.99 (d, 2H); 7.91 (dd, 2H); 7.83 (d, 2H); 7.66 (m, 3H); 7.55 (d, 1H); 7.42 (t, 2H); 7.20 (m, 1H) ppm. FD-MS: *m/z* 790.82 ([M-2PF₆-H]⁺). ESI-MS: *m/z* 937.3 ([M-PF₆]⁺), 791.3 ([M-2PF₆-H]⁺), 396.1 ([M-Ru(bpy)₂(PF₆)₂]⁺). MALDI-TOF-MS: *m/z* 791.28 ([M-2PF₆-H]⁺).

C4: 27.2 mg (7.99×10^{-5} mol) of **6a** and 44 mg (8.39×10^{-5} mol) of Ru(bpy)₂Cl₂ were used. An orange solid was obtained. Yield: 72.2 mg (91%). Anal. Calcd for C₃₇H₂₆F₁₂N₈OP₂Ru: C, 44.90; H, 2.65; N, 11.30. Found: C, 44.35; H, 2.85; N, 11.30. ¹H NMR ((CD₃)₂CO): δ = 9.07 (d, 2H); 8.86 (dd, 4H); 8.35 (m, 2H); 8.25

(t, 3H); 8.16 (m, 4H); 7.91 (m, 4H); 7.64 (m, 2H); 7.40 (m, 2H); 7.33 (s, 1H); 6.76 (s, 1H) ppm. MALDI-TOF-MS: m/z 699.73 ([M-2PF₆-H]⁺), 543.71 ([M-2PF₆-bpy-H]⁺)

C5: 25 mg (6.18×10^{-5} mol) of **6b** and 33.8 mg (6.49×10^{-5} mol) of Ru(bpy)₂Cl₂ were used. An orange solid was obtained. Yield: 60.0 mg (91%). Anal. Calcd for C₄₁H₂₈F₁₂N₈OP₂RuS: C, 45.95; H, 2.65; N, 10.45; S, 3.00. Found: C, 45.90; H, 2.65; N, 10.60; S, 2.60. ¹H NMR ((CD₃)₂CO): δ = 8.82 (m, 5H); 8.40 (m, 1H); 8.23-8.16 (m, 8H); 7.96 (m, 2H); 7.64-7.40 (m, 8H); 7.15 (s, 1H); 6.95 (s, 1H) ppm. MALDI-TOF-MS: m/z 781.79 ([M-2PF₆-H]⁺), 625.73 ([M-2PF₆-bpy-H]⁺), 368.73 ([M-Ru(bpy)₂(PF₆)₂]⁺)

C6: 23.5 mg (5.64×10^{-5} mol) of **6c** and 30.8 mg (5.93×10^{-5} mol) of Ru(bpy)₂Cl₂ were used. An orange solid was obtained. Yield: 57.8 mg (96%). Anal. Calcd for C₄₃H₃₀F₁₂N₈OP₂Ru: C, 48.45; H, 2.85; N, 10.50. Found: C, 48.35; H, 3.00; N, 9.90. ¹H NMR ((CD₃)₂CO): δ = 8.83 (m, 5H); 8.40 (m, 1H); 8.25-8.16 (m, 8H); 8.02 (m, 3H); 7.79 (s, 3H); 7.72 (s, 2H); 7.45-7.38 (m, 5H); 7.12 (s, 1H) ppm. MALDI-TOF-MS: m/z 775.65 ([M-2PF₆-H]⁺), 619.62 ([M-2PF₆-bpy-H]⁺), 463.57 ([M-(bpy)₂-2PF₆-H]⁺), 362.67 ([M-Ru(bpy)₂(PF₆)₂]⁺)

Insert Scheme 2 at about here

Results and Discussion

Synthesis. In order to compare the effect of the electronic nature of aryl and heteroaryl moieties on the optical properties of linear imidazo-phenanthrolines **4-6**, formyl- derivatives containing bithienyl **1a-b**, arylthienyl **2**, furyl **3a**,

thienylfuryl **3b** and arylfuryl **3c** π -conjugated bridges were used as precursors of phenanthrolines **4-6**. Compounds **1a**, **2**, **3a** and **3c** were commercially available. The synthesis of 5'-formyl-2-methoxy-2,2'-bithiophene **1b** has been reported.²⁰ Therefore, heterocyclic ligands **4-6** with either bithienyl, arylthienyl, furyl, thienylfuryl and arylfuryl moieties (unsubstituted or bearing a methoxy donor group) linked to the chelating imidazo-phenanthroline system, were synthesized in good to excellent yields (60-85%, Table 1) through the Radziszewski reaction,²¹ using 5,6-phenanthroline-dione, formyl precursors **1-2** and ammonium acetate in refluxing glacial acetic acid for 15 h (Scheme 1).

In the ¹H NMR spectra of most imidazo-phenanthroline derivatives, a peak at about 13.8-13.9 ppm was detected as a broad singlet that was attributed to the N-H in the imidazole moiety. The NH was also identified by IR spectroscopy as a sharp band within the spectral region of 3371-3439 cm⁻¹.

Insert Table 1 at about here

The complexes were obtained by direct reaction of the ligands with Ru(bpy)₂Cl₂ in ethylene glycol, under microwave irradiation for 2 min. Their purity was confirmed by elemental analysis, ¹H NMR and MALDI-TOF MS (see Experimental section).

Spectroscopic characterization. The absorption spectra of the Ru(II) complexes consist mainly of three resolved bands in the 200-600 nm region. The bands around 280 nm are attributed to ligand-centered (LC) π - π^* transitions; the bands around 350 nm can either be due to the n- π^* transitions or

inter-ligand $\pi-\pi^*$ transitions, and the lowest energy bands at around 460 nm are assigned to the metal-to-ligand charge transfer (MLCT) transitions. The emission spectra are all centered above 600 nm according to what is expected for Ru(II) polypyridyl complexes (see Figures S1 and S2, Supplementary material). Table 2 summarizes all the spectroscopic data.

Insert Table 2 at about here

Interaction of Ru(II) complexes with DNA. Electronic absorption spectroscopy is a very useful technique in DNA-binding studies, since binding to double stranded (ds) DNA through intercalation normally results in hypochromism and bathochromism of the MLCT visible absorption band of the complex.²² The extent of the hypochromism usually parallels the intercalative binding strength.²² On the other hand, luminescence studies usually show the enhancement of both the luminescence intensity and lifetime of the Ru(II) complexes upon binding to the DNA. This indicates that the complexes can interact with DNA and are protected by this polynucleotide to some extent from quenching by molecular oxygen and the solvent molecules. Emission quenching experiments may provide further information, since the Stern-Volmer quenching constants can be used as a measure of the binding affinity.

In this way, preliminary studies were performed with complexes **C1**, **C2** and **C3** to compare the interaction of these complexes with DNA in a qualitative way. All the preliminary results obtained with **C1** to **C3** in the presence of DNA are reported in the Supplementary material.

The interaction of the stronger emissive **C3** to **C6** complexes was studied quantitatively; Figure 1 shows in more detail the spectroscopic study of complex **C3** bearing a thienyl-aryl substituent in the presence of increasing amounts of DNA. Figure 1A indicates that there is a hypochromicity in the MLCT band upon addition of DNA, suggesting the intercalation of **C3** into the double DNA helix. At the same time the emission intensity (Figure 1B) and lifetime (Table T1 in Supplementary Material) of the bound luminophore are enhanced due to a combination of a more hydrophobic microenvironment around the metal complex after binding (the O-H oscillators help to deactivate the emissive ³MLCT state)⁸ and the protection from quenching by dissolved molecular oxygen imparted by the polynucleotide strand. Inset in Figure 1B shows the increases observed both in the steady state spectra and in the luminescence lifetime in the presence of DNA.

Insert Figure 1 at about here

A similar behavior was found for the other imidazo-phenanthroline complexes, as can be seen for complex **C5** in Figure 2 and Table T2 in Supplementary Material. All the results for the remaining complexes are reported in Figures S3 to S6, and Tables T3 and T4, Supplementary Material.

Insert Figure 2 at about here

The intrinsic DNA binding constants (K_b), which provide a measure of the interaction strength, were obtained by monitoring the changes in absorbance at 460 nm with increasing concentrations of DNA. The experimental data were fit

to the simple Scatchard eq (2),²³ that is only valid for low binder-to-DNA ratios (i.e., far from the DNA saturation) and assumes no binding cooperativity:

$$[\text{DNA}]/(\epsilon_a - \epsilon_f) = [\text{DNA}]/(\epsilon_b - \epsilon_f) + 1/[K_b(\epsilon_b - \epsilon_f)] \quad (2)$$

where $[\text{DNA}]$ is the concentration of the nucleic acid in base pairs, ϵ_a is the apparent absorption coefficient obtained by calculating $A_{\text{obs}}/[\text{Ru}]$, and ϵ_f and ϵ_b are the absorption coefficients for the free and the fully bound ruthenium complex, respectively.

In the $[\text{DNA}]/(\epsilon_a - \epsilon_f)$ vs. $[\text{DNA}]$ plot, K_b is given by the ratio of the slope to the intercept. The binding constants obtained thereof for complexes **C3**, **C4**, **C5** and **C6** were, respectively, 2.7×10^5 , 3.0×10^5 , 1.3×10^5 and $1.6 \times 10^5 \text{ M}^{-1}$ (see Figures S7 to S10, Supplementary Material). These values are larger than those of the DNA (minor) groove binding Ru(II) complexes such as tris(1,10-phenanthroline)ruthenium(II) and related structures ($1.1 \times 10^4 - 4.8 \times 10^4 \text{ M}^{-1}$),^{23,24,25} but smaller than those observed for the $[\text{Ru}(\text{bpy})_2(\text{dppz})]^{2+}$ DNA intercalator and other complexes containing an extended phenazine ligand (10^7 to 10^9 M^{-1}).^{4c} This result would indicate a more intimate binding of the imidazo-phenanthroline complex to the polynucleotide double strand than that of the simple tris-phenanthroline complex although not as efficient as those bearing a fused polycyclic (hetero)aromatic system that can be inserted between adjacent base pairs of the DNA ladder.

It is interesting to note that the MLCT absorption band of complexes **C4-C6** centered at ca. 455 nm undergoes a more pronounced hypochromic effect upon binding to ds-DNA than the MLCT band at ca. 430 nm. This observation would indicate that the former corresponds to the electronic transition involving the chelating ligand that interacts more closely with the polynucleotide base-pair

strand, presumably the intercalated **6a-c** imidazo-phenanthrolines (the small bpy ligands are unable to intercalate into the double helix²⁶). Surprisingly enough, the same difference is not observed for the Ru(II) complex **C3** that contains the imidazo-phenanthroline **5**. In the absence of molecular modeling studies, we can hypothesize that the crescent-shaped ligands 6a-c intercalate more efficiently than the long, linear, twisted phenyl-substituted imidazo-phenanthroline **5**.

Except for **C3**, the emission profile of the luminophoric complexes in buffer solution can only be fit to a double exponential function (Tables T1 to T4, Supplementary Material). This fact may be attributed to aggregation of the hydrophobic dyes; the observation of just two components is a consequence of the strong fitting power of the bi-exponential function which does not require introduction of additional components. However, a variety of self-aggregates displaying different stoichiometries is to be expected, the emission lifetime of which cannot be fully resolved. In the presence of just a 5-fold (molar) concentration of DNA the luminescence decay slows down for the same reasons outlined above for the emission intensity and, although the individual lifetimes of the observed components remain almost the same for higher DNA concentrations, τ_m increases as a consequence of the rise of the contribution of the long lifetime component to the overall decay (except for **C3** where the individual components remain unchanged). These results indicate that the Ru(II) complexes in buffer solution are already fully bound to the DNA under the used experimental conditions even at a $[DNA]_{bp}/Ru$ ratio as low as 5. Further addition of the polynucleotide would just make the luminescent probes shift their binding mode, e.g. from aggregated on the double helix to individually bound,

as they become “diluted” with larger amounts of DNA. The longest emission lifetime would correspond to the isolated Ru(II) complexes while the shortest one is the signature of the aggregates. The lack of change in the relative contribution of the short and long lifetimes in the case of the DNA-bound complex **C3**, and the preeminence of the fast component of the decay even at large $[\text{DNA}]_{\text{bp}}/\text{Ru}$ ratios might be a consequence of its different interaction mode with the polynucleotide (see above) and a more difficult self-aggregation (unlike the other imidazo-phenanthroline complexes, a single-exponential decay is observed for the photoexcited **C3** in the absence of DNA).

Emission quenching studies. After having studied the interaction of all the complexes with DNA, it was observed that in all cases no significant changes occurred, neither in the emission spectra nor in the luminescence lifetimes, for DNA/Ru ratios in excess of 30. Therefore, this ratio was chosen for subsequent studies with selected excited state quenchers (ethidium bromide, potassium hexacyanoferrate(II) and methyl viologen).²⁷ It is well established that those quenchers deactivate the excited state of most Ru(II) polypyridyls by photoinduced electron transfer with rate constants in excess of $10^9 \text{ L mol}^{-1} \text{ s}^{-1}$. Starting with **C3**, it was found out that the addition of increasing amounts of ethidium bromide to a mixture of **C3**+DNA (ratio 1:30) promoted an enhancement of the absorption values in the region corresponding to the MLCT absorption band (Figure S11, Supplementary Material). However, since the intrinsic absorption of ethidium takes place in the same wavelength range, this absorption increase had to be discarded. A similar effect occurred with the emission spectra (Figure S11, Supplementary Material) and luminescence

lifetime measurements (Table T5, Supplementary Material), since both compounds emit in the same region, and the lifetime values for ethidium are significantly shorter, thus masking the true τ_m values.

In the case of potassium hexacyanoferrate(II) quencher, no changes in the luminescence lifetime were observed for the photoexcited **C3** bound to DNA (See Figure S12 and Table T6, Supplementary Material). These results suggest that the complex is fully bound to DNA as the positively charged complex should be easily quenched by this highly anionic quencher if both species were free in solution,²⁷ while the negative DNA phosphate backbone hinders quenching of the bound complex emission. However, total luminescence quenching is observed for the DNA-bound **C3** complex, both in steady-state and time-resolved emission, in the presence of methyl viologen (MV^{2+}) (Figure 3 and Table 3).

Insert Figure 3 and Table 3 at about here

Emission quenching experiments for complexes **C4**, **C5** and **C6** have also been performed using methyl viologen as a quencher, and the results are comparable to those obtained for **C3**. Steady-state emission spectra and luminescence lifetime decays for **C5** are represented on Figure 4 and Table 4, respectively (See absorption spectra in Figure S13, Supplementary Material). All the results for the remaining complexes are reported in Figures S14 and S15 and Tables T7 and T8, Supplementary Material. The slight enhancement of the lifetime values for the last methyl viologen additions (Tables T7 and T8) suggest a partial displacement of the DNA bound Ru(II) complexes to the bulk solution under these conditions.

Insert Figure 4 and Table 4 at about here

From the complexes **C3-C6** emission quenching studies with methyl viologen the Stern-Volmer constants, K_{SV} , and the corresponding quenching rate constants, k_q , were determined. Whenever non-linear Stern-Volmer plots were obtained, the rate constant data refer to the initial slope. The k_q values obtained from each lifetime component (fast and slow, respectively) of each complex, were: 1.7×10^{11} and $1.0 \times 10^{11} \text{ M}^{-1}\text{s}^{-1}$ (**C3**); 9.4×10^9 and $1.9 \times 10^{10} \text{ M}^{-1}\text{s}^{-1}$ (**C4**); 3.9×10^9 and $7.6 \times 10^9 \text{ M}^{-1}\text{s}^{-1}$ (**C5**); 2.0×10^{10} and $2.1 \times 10^{10} \text{ M}^{-1}\text{s}^{-1}$ (**C6**). These values exceed by one or two orders of magnitude those commonly obtained for Ru(II) complexes with MV^{2+} (ca. $10^9 \text{ M}^{-1}\text{s}^{-1}$).²⁷ Such acceleration of the photoinduced electron transfer might be due to several factors, one of them being the increase of the local concentration (closer average distance) of donor and acceptor species on the nucleic acid (since both the ruthenium (II) complex and the quencher are bound to the DNA). Considering this effect, the calculated values for the quenching rate constants represent only apparent values, since the quencher concentration values on the abscissa correspond to different local quencher concentrations on the polynucleotide.

The results for **C3+DNA** in the presence of methyl viologen are represented in Figure 5. All the other results, including the data for C3 with ethidium bromide, are represented in Figures S16 to S19, Supplementary Material).

Insert Figure 5 at about here

Conclusions

Four new ligands and six Ru(II) polypyridyl complexes have been synthesized, the latter through microwave-assisted reactions, which considerably reduces the reaction times from hours to minutes, with satisfactory yields. Studies of their interaction with calf thymus DNA have suggested a partial intercalation of the probes into the nucleic acid double strand. According to the structural features of the complexes and the obtained values for the binding constants, it is possible that the crescent-shaped complexes C4, C5 and C6 have a more intimate binding to the polynucleotide double strand than the phenyl-substituted C3. Luminescence quenching studies further support this hypothesis, since in the case of potassium hexacyanoferrate(II) no quenching was observed (which indicates that all the complex was bound to the DNA) and with methyl viologen the quenching was accompanied by partial displacement of the complexes to the bulk solution at high quencher concentrations. All these results illustrate the feasibility of fine tuning the DNA interaction mode of luminescent Ru(II) complexes containing extended imidazo-phenanthroline ligands by molecular engineering of their aryl substituents. Such feature might be used in the future to design tailored molecular probes of the polynucleotide features.

Acknowledgment

We are indebted to InOU Uvigo by project K914 122P 64702 (Spain), Xunta de Galicia (Spain) by project 09CSA043383PR and FCT-Portugal by project PTDC/QUI/66250/2006 (FCOMP-01-0124-FEDER-007428), for financial support. The NMR spectrometers are part of the National NMR Network

and were purchased in the framework of the National Programme for Scientific Re-equipment, contract REDE/1517/RMN/2005, with funds from POCI 2010 (FEDER) and FCT-Portugal.

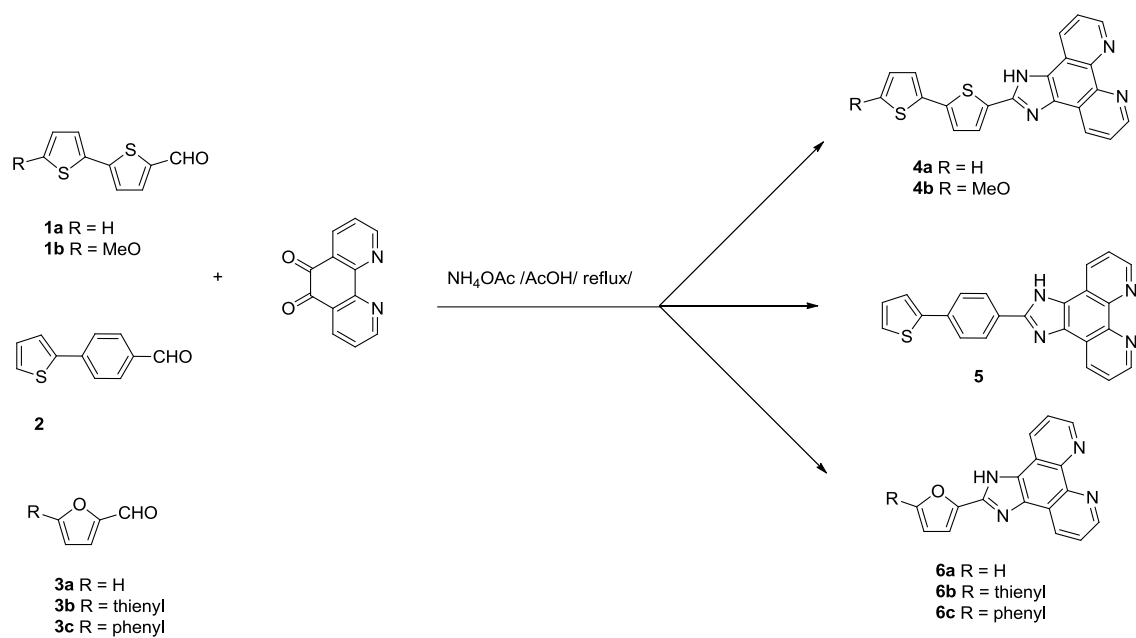
J. L. C. and C. L. thank Xunta de Galicia, Spain, for the Isidro Parga Pondal Research Program. B. P. and R. B. thank FC-MCTES (Portugal) for their PhD grants SFRH/BD/27786/2006 and SFRH/BD/36396/2007, respectively.

We are grateful to Dr. A. Jorge Parola from the REQUIMTE, Universidade NOVA de Lisboa, Portugal for his help with the synthesis of the Ru(bpy)₂Cl₂ precursor.

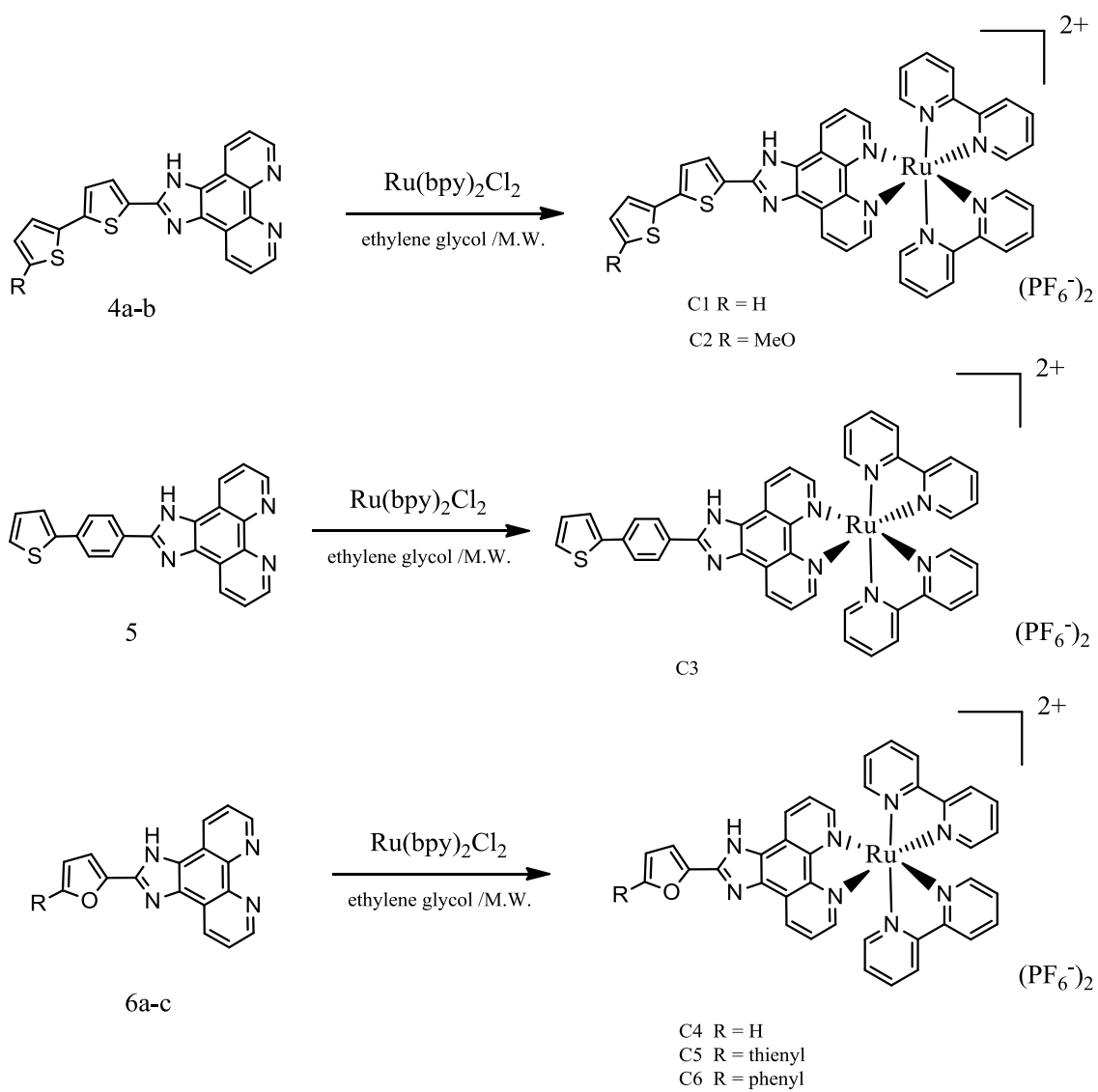
Supporting Information Available

Absorption spectra of **C1** to **C6** complexes; luminescence lifetimes for **C3** to **C6** at different ratios Ru:DNA; Absorption and emission spectra of **C4** and **C6** with CT-DNA; Ethidium bromide, methyl viologen and potassium ferrocyanide experiments and Stern-Volmer experiments with DNA. This material is available free of charge via the Internet at <http://pubs.acs.org>.

Schemes, Tables and Figures



Scheme 1. Synthesis of imidazo-furyl and imidazo-thienyl-phenanthroline derivatives.



Scheme 2. Synthesis of Ruthenium(II) Complexes.

Formyl derivative	Phenanthroline product	R	Yield (%)	IR $\nu_{\text{N-H}}$ (cm^{-1}) ^a	δ_{H} (imidazole) (ppm) ^d
2	5	-	82	3439 ^b	13.8
3a	6a	H	85	3396	13.9
3b	6b	thienyl	79	3436 ^c	13.9
3c	6c	phenyl	60	3371	- ^e

Table 1. Yields, IR absorption spectra and ¹H RMN spectra of phenanthrolines **5-6**.

^a For the NH stretching band (recorded in Nujol).

^b For the NH stretching band (recorded in KBr).

^c For the NH stretching band (recorded in liquid film).

^d For the NH proton of the imidazole ring for compounds **5-6** (DMSO-d₆).

^e Not observed.

Complex	λ_{max}^{abs} / nm	$\epsilon_{max} / M^{-1}cm^{-1}$	λ_{max}^{em} / nm	Φ_F
C1	463	12700	608	0.006
C2	459	17800	607	0.015
C3	460	11900	603	0.016
C4	459	15900	613	0.009
C5	458	14300	613	0.008
C6	457	12000	611	0.008

Table 2 – MLCT (d- π^*) absorption and emission maxima, molar absorption coefficients (in Tris buffer) and fluorescence quantum yields (in air-equilibrated DMSO) of complexes **C1** to **C6**.

[MV ²⁺] / μM	$\tau_1/\mu\text{s}$ (%)	$\tau_2/\mu\text{s}$ (%)	$\tau_3/\mu\text{s}$ (%)	$\tau_m / \mu\text{s}$	χ^2
0	-	0.74 67	1.34 33	0.94	1.10
5	0.14 21	0.43 60	0.84 19	0.45	1.04
15	0.08 37	0.22 50	0.54 13	0.21	1.03
25	0.08 56	0.21 37	0.55 10	0.17	1.10
50	0.04 54	0.13 41	0.40 5	0.10	1.04
75	0.03 62	0.10 35	0.38 3	0.07	1.05
100	0.03 69	0.09 30	0.44 1	0.05	0.91
125	0.02 66	0.08 32	0.40 2	0.05	1.04
150	0.02 70	0.07 29	0.40 1	0.04	0.95
175	0.02 73	0.07 25	0.41 2	0.04	0.98
200	0.02 77	0.07 22	0.47 1	0.04	0.98

Table 3 – Luminescence lifetimes of 1:30 C3:DNA at different MV²⁺ concentrations. [C3] = 4.90 μM . λ_{exc} = 405 nm. λ_{em} = 610 nm. [DNA]_{stock} = 2.82 mM. [MV²⁺]_{stock} = 5 mM.

[MV ²⁺] / μM	$\tau_1/\mu\text{s}$ (%)	$\tau_2/\mu\text{s}$ (%)	$\tau_3/\mu\text{s}$ (%)	$\tau_m / \mu\text{s}$	χ^2
0	-	0.50 47	1.51 53	1.04	1.03
25	0.18 32	0.49 61	1.09 7	0.43	1.12
50	0.13 32	0.31 55	0.67 13	0.30	1.19
75	0.12 57	0.36 40	0.85 3	0.24	1.11
100	0.07 40	0.21 43	0.55 17	0.21	1.12
150	0.07 57	0.31 34	0.65 9	0.20	1.09
200	0.05 55	0.28 27	0.57 18	0.21	1.06

Table 4 – Luminescence lifetimes of 1:30 **C5**:DNA at different MV²⁺ concentrations. [C5] = 10.5 μM . λ_{exc} = 405 nm. λ_{em} = 613 nm. [DNA]_{stock} = 2.02 mM. [MV²⁺]_{stock} = 5 mM.

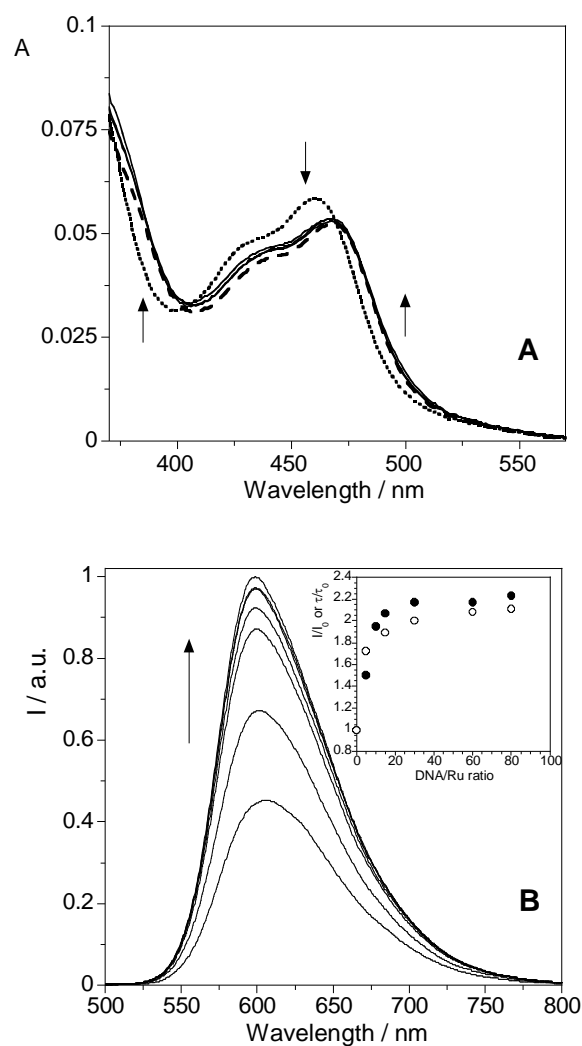


Figure 1 – (A) Absorption spectra of **C3**, 4.9 μM in TRIS buffer, in the absence (···), and in the presence of CT-DNA in ratios of 5 (---) and 10 to 30 (—). **(B)** Emission spectra of C3, 4.9 μM in TRIS buffer, in the presence of increasing amounts of CT-DNA (DNA/Ru ratio of 0 – 80, in base pairs). $\lambda_{\text{exc}} = 465 \text{ nm}$. Inset: changes in the emission intensity, I/I_0 (●), and emission lifetime, τ/τ_0 (○), of C3 as a function of DNA/Ru ratio.

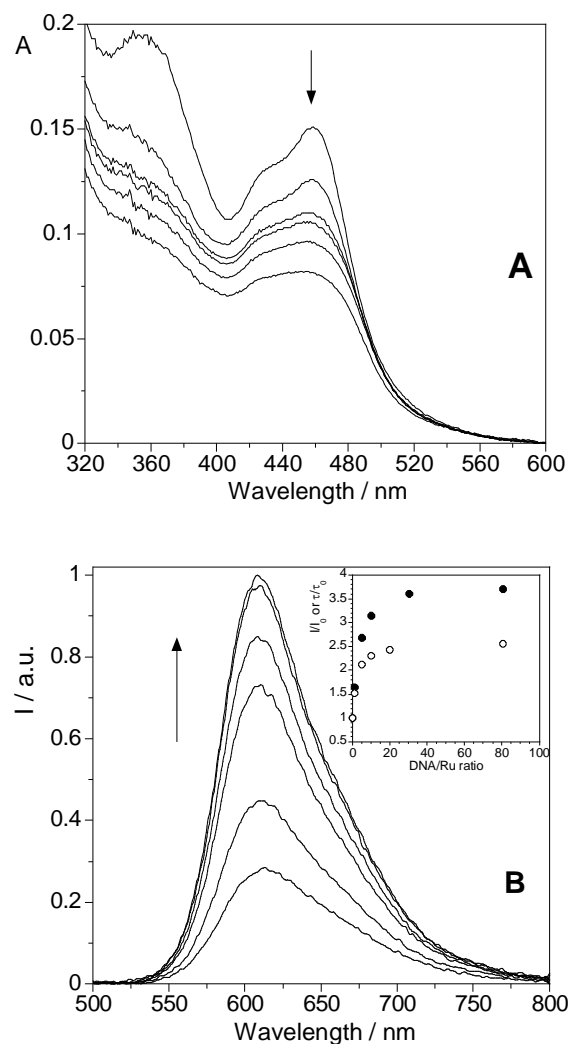


Figure 2 – (A) Absorption spectra of C5, 10.5 μM in TRIS buffer, in the presence of increasing amounts of CT-DNA (DNA/Ru ratio of 0 – 80, in base pairs). **(B)** Emission spectra of C5, 10.5 μM in TRIS buffer, in the presence of increasing amounts of CT-DNA (DNA/Ru ratio of 0 – 80, in base pairs). $\lambda_{\text{exc}} = 460$ nm. Inset: changes in the emission intensity, I/I_0 (\bullet), and emission lifetime, τ/τ_0 (\circ), of C5 as a function of DNA/Ru ratio.

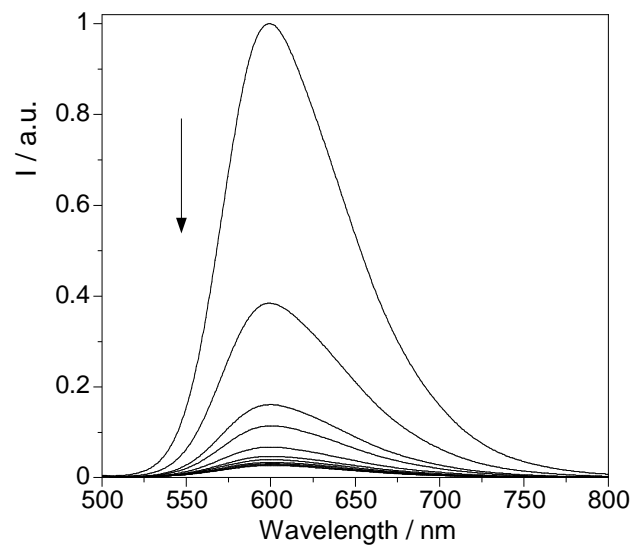


Figure 3 – Emission spectra of CT-DNA + **C3** (Ratio 30/1) in the presence of increasing amounts of methyl viologen (0 – 200 μM). $[\text{C3}] = 4.90 \mu\text{M}$. $[\text{DNA}]_{\text{stock}} = 2.82 \text{ mM}$. $[\text{MV}^{2+}]_{\text{stock}} = 5 \text{ mM}$. $\lambda_{\text{exc}} = 465 \text{ nm}$.

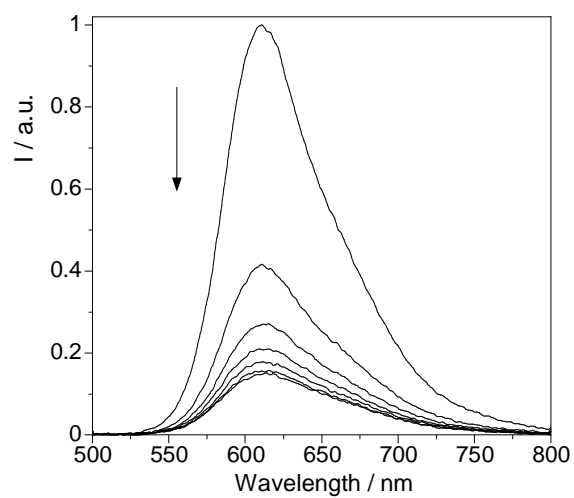


Figure 4 – Emission spectra of CT-DNA + **C5** (Ratio 30/1) in the presence of increasing amounts of methyl viologen (0 – 200 μM). $\lambda_{\text{exc}} = 465 \text{ nm}$. $[\text{C5}] = 10.5 \mu\text{M}$. $[\text{DNA}]_{\text{stock}} = 2.02 \text{ mM}$. $[\text{MV}^{2+}]_{\text{stock}} = 5 \text{ mM}$.

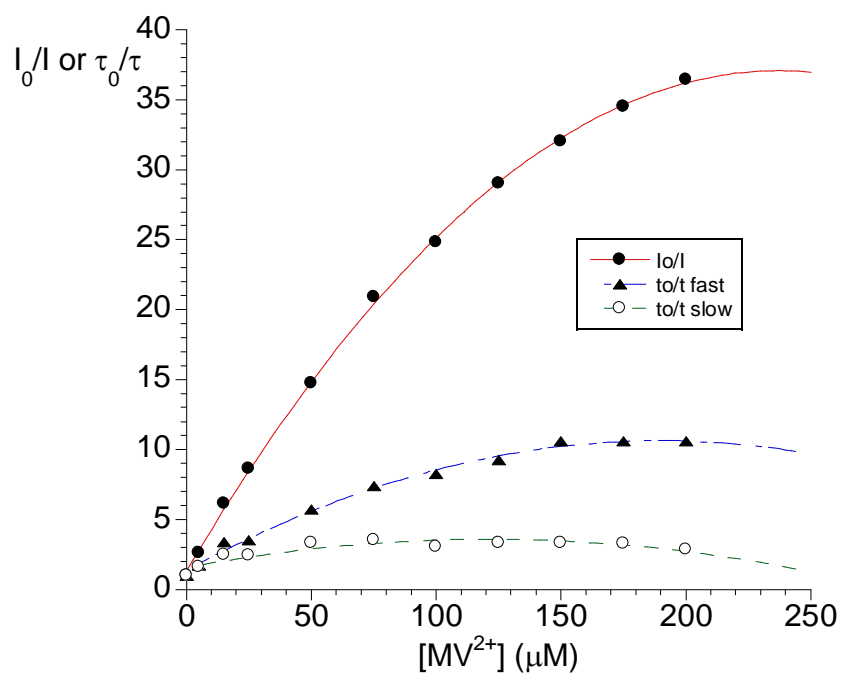


Figure 5 – Stern-Volmer emission intensity (●) and lifetime quenching plot for C3+DNA (ratio 1:30) in the presence of increasing amounts of methyl viologen (MV^{2+}). Both fast (short) (▲) and slow (long) (○) components of the emission decay are represented. $\lambda_{exc} = 405$ nm. Emission collected at 610 nm.

References

(1) (a) J.G. Vos, J.M. Kelly, Dalton Trans. 41 (2006) 4869; (b) D.A. Jose, P. Kar, D. Koley, B. Ganguly, W. Thiel, H. N. Ghosh, A. Das, Inorg. Chem. 46 (2007) 5576; (c) V. Balzani, G. Bergamini, F. Marchioni, P. Ceroni, Coord. Chem. Rev. 250 (2006) 1254; (d) A. Ghosh, P. Das, S. Saha, T. Banerjee, H. B. Bhatt, A. Das, Inorg. Chim. Acta 372 (2011) 115.

(2) (a) B. Norden, P. Lincoln, B. Akerman, E. Tuite, Met. Ions Biol. Syst. 33 (1996) 177; (b) E.D.A. Stemp, J.K. Barton, Met. Ions Biol. Syst. 33 (1996) 325; (c) C. Moucheron, A. Kirsch-De Mesmaeker, J.M. Kelly, Struct. Bonding 92 (1998) 163; (d) K.E. Erkkila, D.T. Odom, J.K. Barton, Chem. Rev. 99 (1999) 2777; (e) L.N. Ji, X.H. Zou, J.G. Liu, Coord. Chem. Rev. 216 (2001) 513; (f) C. Metcalfe, J.A. Thomas, Chem. Soc. Rev. 32 (2003) 215; (g) M.J. Clarke, Coord. Chem. Rev. 232 (2002) 69; (h) H. Chao, L.N. Ji, Bioinorg. Chem. Appl. 3 (2005) 15; (i) A. Ghosh, P. Das, M. R. Gill, P. Kar, M. G. Walker, J. A. Thomas, A. Das, Chem. Eur. J. 17 (2011) 2089.

(3) B.T. Farrer, H.H. Thorp, Inorg. Chem. 39 (2000) 44.

(4) (a) A. Kirsch-De Mesmaeker, J.P. Lecomte, J.M. Kelly, Top. Curr. Chem. 177 (1996) 25; (b) Y. Jenkins, A.E. Friedman, N.J. Turro, J.K. Barton, Biochemistry 31 (1992) 10809; (c) A.E. Friedman, J.C. Chambron, J.P. Sauvage, N.J. Turro, J.K. Barton, J. Am. Chem. Soc. 112 (1990) 4960; (d) A.B. Tossi, J.M. Kelly, Photochem. Photobiol. 49 (1989) 545; (e) I. Ortmans, C. Moucheron, A. Kirsch-De Mesmaeker, Coord. Chem. Rev. 168 (1998) 233; (f)

J.M. Kelly, M. Feeney, L. Jacquet, A. Kirsch-De Mesmaeker, J.P. Lecomte, *Pure Appl. Chem.* 69 (1997) 767; (g) F. Piérard, A. Del Guerso, A. Kirsch-De Mesmaeker, M. Demeunynck, J. Lhomme, *Phys. Chem. Chem. Phys.* 3 (2001) 2911.

(5) (a) E. Amouyal, A. Homsí, J.C. Chambron, J.P. Sauvage, *J. Chem. Soc. Dalton Trans.* (1990) 1841; (b) R.B. Nair, B.M. Cullum, C.J. Murphy, *Inorg. Chem.* 36 (1997) 962; (c) L. Ujj, C.G. Coates, J.M. Kelly, P. Kruger, J.J. McGarvey, G.H. Atkinson, *J. Phys. Chem. B.* 106 (2002) 4854; (d) C.G. Coates, P.L. Callaghan, J.J. McGarvey, J.M. Kelly, P. Kruger, M.E. Higgins, *J. Raman Spectrosc.* 31 (2000) 283; (e) C. Turro, S.H. Bossman, Y. Jenkins, J.K. Barton, N.J. Turro, *J. Am. Chem. Soc.* 117 (1995) 9026; (f) E. Sabatini, H.D. Nikol, H.B. Gray, F.C. Anson, *J. Am. Chem. Soc.* 118 (1996) 1158; (g) X. Q. Guo, F.N. Castellano, L. Li, J.R. Lakowicz, *Biophys. Chem.* 71 (1998) 51; (h) M.K. Brennaman, J.H. Alstrum-Acevedo, C.N. Fleming, P. Jang, T.J. Meyer, J.M. Papanikolas, *J. Am. Chem. Soc.* 124 (2002) 15094; (i) G. Pourtois, D. Beljonne, C. Moucheron, S. Schumm, A. Kirsch-De Mesmaeker, R. Lazzaroni, J.L. Brédas, *J. Am. Chem. Soc.* 126 (2004) 683.

(6) E.J.C. Olson, D. Hu, A. Hormann, A.M. Jonkman, M.R. Arkin, E.D.A. Stemp, J.K. Barton, P.F. Barbara, *J. Am. Chem. Soc.* 119 (1997) 11458.

(7) (a) E. Tuite, P. Lincoln, B. Nordén, *J. Am. Chem. Soc.* 119 (1997) 239; (b) C. Hiort, P. Lincoln, B. Nordén, *J. Am. Chem. Soc.* 115 (1993) 3448; (c) P. Lincoln, A. Broo, B. Nordén, *J. Am. Chem. Soc.* 118 (1996) 2644; (d) P. Nordell,

F. Westerlund, M. Wilhelmsson, B. Nordén, P. Lincoln, *Angew. Chem. Int. Ed.* 46 (2007) 2203; (e) P. Nordell, P. Lincoln, *J. Am. Chem. Soc.* 127 (2005) 9670; (f) B. Önfelt, J. Olofsson, P. Lincoln, B. Nordén, *J. Phys. Chem. A* 107 (2003) 1000; (g) J. Olofsson, B. Önfelt, P. Lincoln, *J. Phys. Chem. A* 108 (2004) 4391; (h) F. Westerlund, F. Pierard, M.P. Eng, P. Nordén, P. Lincoln, *J. Phys. Chem. B* 109 (2005) 17327; (i) F. Westerlund, M.P. Eng, M.U. Winters, P. Lincoln, *J. Phys. Chem. B* 111 (2007) 310; (j) F. Westerlund, P. Nordell, J. Blechinger, T.M. Santos, B. Nordén, P. Lincoln, *J. Phys. Chem. B* 112 (2008) 6688; (k) C.G. Coates, J. Olofsson, M. Coletti, J.J. McGarvey, B. Önfelt, P. Lincoln, B. Norden, E. Tuite, P. Matousek, A.W. Parker, *J. Phys. Chem. B* 105 (2001) 12653; (l) M. Li, P. Lincoln, *J. Inorg. Biochem.* 103 (2009) 963; (m) A. Ghosh, A. Mandoli, D. K. Kumar, N. S. Yadav, T. Ghosh, B. Jha, J. A. Thomas, A. Das, *Dalton Trans.* (2009) 9312.

(8) (a) D. García-Fresnadillo, G. Orellana, *Helv. Chim. Acta* 84 (2001) 2708; (b) S.W. Snyder, S.L. Buell, J.N. Demas, B.A. DeGraff, *J. Phys. Chem.* 93 (1989) 5265.

(9) (a) A. Hergueta-Bravo, M.E. Jiménez-Hernández, F. Montero, E. Oliveros, G. Orellana, *J. Phys. Chem. B* 106 (2002) 4010; (b) M.F. Ottaviani, N.D. Ghatlia, S.H. Bossmann, J.K. Barton, H. Durr, N.J. Turro, *J. Am. Chem. Soc.* 114 (1992) 8946.

(10) M.R. Gill, J. Garcia-Lara, S.J. Foster, C. Smythe, G. Battaglia, J.A. Thomas, *Nature Chemistry* 1 (2009) 662.

(11) A. Kirsch-De Mesmaeker, G. Orellana, J.K. Barton, N.J. Turro, *Photochem. Photobiol.* 52 (1990) 461.

(12) J.M. Kelly, A.B. Tossi, D.J. McConnell, C. OhUigin, *Nucl. Acids Res.* 13 (1985) 6017.

(13) (a) C. Lodeiro, J.L. Capelo, J.C. Mejuto, E. Oliveira, H.M. Santos, B. Pedras, C. Nuñez, *Chem. Soc. Rev.* 39 (2010) 2948; (b) C. Lodeiro, F. Pina, *Coord. Chem. Rev.* 253 (2009) 1353; (c) B. Pedras, H.M. Santos, L. Fernandes, B. Covelo, A. Tamayo, E. Bértolo, J.L. Capelo, T. Avilés, C. Lodeiro, *Inorg. Chem. Comm.* 10 (2007) 925; (d) J. Lopez-Gejo, A. Arranz, A. Navarro, C. Palácio, E. Munoz, G. Orellana, *J. Am. Chem. Soc.* 132 (2010) 1746; (e) J. Lopez-Gejo, D. Haigh, G. Orellana, *Langmuir* 26 (2010) 2144.

(14) (a) R.M.F. Batista, S.P.G. Costa, C. Lodeiro, M. Belsley, M.M.M. Raposo, *Tetrahedron* 64 (2008) 9230. (b) R.M.F. Batista, S.P.G. Costa, C. Lodeiro, M. Belsley, E. de Matos Gomes, M.M.M. Raposo, *Adv. Mat. Forum IV* 263 (2008) 587.

(15) R.M.F. Batista, S.P.G. Costa, M. Belsley, M.M.M. Raposo, *Dyes Pigments* 80 (2009) 329.

(16) A. Kobori, J. Morita, M. Ikeda, A. Yamayoshi, A. Murakami, *Biorg. Med. Chem. Lett.* 19 (2009) 3657.

-
- (17) L.F. Tan, S. Zhang, X.H. Liu, Y.Xiao, *Australian J. Chem.* 9 (2008) 725.
- (18) G. Orellana, A. Kirsch-De Mesmaeker, J.K. Barton, N.J. Turro, *Photochemistry and Photobiology* 54 (1991) 499.
- (19) B.P. Sullivan, D.J. Salmon, T.J. Meyer, *Inorg. Chem.* 17 (1978) 3334.
- (20) M.M.M. Raposo, G. Kirsch, *Tetrahedron* 59 (2003) 4891.
- (21) D. Davidson, M. Weiss, M.J. Jelling, *J. Org. Chem.* 2 (1937) 319.
- (22) E.C. Long, J.K. Barton, *Acc. Chem. Res.* 23 (1990) 271.
- (23) A. Wolf, G.H. Shimer Jr., T. Meehan, *Biochemistry* 26 (1987) 6392.
- (24) A.M. Pyle, J.P. Rehmman, R. Meshoyrer, C.V. Kumar, N.J. Turro, J.K. Barton, *J. Am. Chem. Soc.* 111 (1989) 3051.
- (25) J.L. Morgan, D.P. Buck, A.G. Turley, J.G. Collins, F.R. Keene, *Inorg. Chim. Acta* 359 (2006) 888.
- (26) I.D. Vladescu, M.J. McCauley, M.E. Nuñez, I. Rouzina, M.C. Williams, *Nature Methods* 4 (2007) 517.

(27) M.Z. Hoffman, F. Bolletta, L. Moggi, G.L. Hug, J. Phys. Chem. Ref. Data 18
(1989) 219.